Article

pubs.acs.org/Biomac

Recombinant Production, Characterization, and Fiber Spinning of an Engineered Short Major Ampullate Spidroin (MaSp1s)

Christopher Thamm[†] and Thomas Scheibel*[,†,‡,§,∥,⊥,#]

[†]Lehrstuhl Biomaterialien, Fakultät für Ingenieurwissenschaften and [‡]Bayreuther Zentrum für Kolloide und Grenzflächen (BZKG), Universität Bayreuth, Universitätsstraße 30, 95440 Bayreuth, Germany

[§]Bayerisches Polymerinstitut (BPI), Universitätsstraße 30, 95440 Bayreuth, Germany

[∥]Bayreuther Zentrum für Molekulare Biowissenschaften (BZMB), [⊥]Institut für Bio-Makromoleküle (bio-mac), and [#]Bayreuther Materialzentrum (BayMAT), Universität Bayreuth, Universitätsstraße 30, 95440 Bayreuth, Germany

Supporting Information

ABSTRACT: Spider dragline silk exhibits an extraordinary toughness and is typically composed of two types of major ampullate spidroins (MaSp1 and MaSp2), differing in their proline content and hydrophobicity. In this paper, we recombinantly produced an unusual but naturally occurring short major ampullate spidroin (MaSp1s) as a fusion construct between established *Latrodectus hesperus* terminal domains and the novel *Cyrtophora moluccensis* core domain. The sequence of the recombinant spidroin was engineered to guarantee high yields upon recombinant production and was named eMaSp1s. Its solution structure as well as the mechanical properties of wet-spun eMaSp1s fibers were examined. Structural characterization using CD- and FTIR spectroscopy showed a predominantly α-helical solution structure and a high ß-sheet content within fibers. Surprisingly, eMaSp1s fibers show similar mechanical properties as wet-spun fibers of other engineered spider silk proteins, albeit eMaSp1s has a lower molecular weight and not the typical sequence repeats in its core domain. Therefore, the findings provide insights into the molecular interplay necessary to obtain the typical silk fiber mechanics.

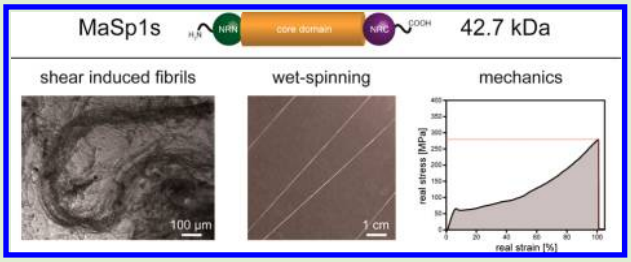

INTRODUCTION

Females of weaving spiders such as *Cyrtophora moluccensis* (orb-weaver) or *Latrodectus hesperus* (cob-weaver) are able to produce up to seven different types of silk,[1] among which the major ampullate (MA) silk (dragline silk) is the best investigated type. MA silk combines good tensile strength and extensibility, leading to a high toughness exceeding that of most natural or synthetic fibers.[2−6] The underlying proteins, called spidroins, originate from the major ampullate gland and comprise two classes, major ampullate spidroin 1 and 2 (MaSp1, MaSp2).[7−9] MaSp have on average a molecular weight of 250−350 kDa, and both classes can be distinguished by their proline content.[10,11] While MaSp1 is more hydrophobic and poor in proline residues, MaSp2 is more hydrophilic and proline-rich.[11−13] Interestingly, the ratio of MaSp1 and MaSp2 greatly differs between spider species, and a putative impact on fiber mechanics has been previously considered.[10,14]

All known MA spidroins share the same architecture with a repetitive intrinsically unstructured core domain (90% of the protein's sequence with up to 100 repeats of highly conserved sequence motifs, each comprising 40−200 amino acids) flanked by folded (five helix bundles), nonrepetitive amino- (NRN) and carboxy-terminal (NRC) domains (100−150 amino acids).[7,15,16] The sequence motifs of the repetitive domains include polyalanine stretches (typically 4−9 alanines) forming ß-sheets upon fiber assembly providing the basis for their identified high tensile strength,[17] and glycine-rich areas ($(GGX)_n$, GPGXX, X = Y, L, or Q) generating an amorphous matrix, thus being responsible for the elasticity of the spider silk fiber.[18−20] While polyalanine and GGX are ubiquitous, GPGXX is only present in MaSp2.[8,21] In contrast to the repetitive domain whose sequence varies between different spider species, the terminal domains of spider silk proteins are highly conserved.[7,22−24] Both terminal domains show α-helical secondary structure and are important for controlling spidroin storage as well as fiber assembly with slightly different features and functions.[24−28]

Recently, Han et al. discovered a novel MaSp1 protein in *Cyrtophora moluccensis*, differing from all previously identified MaSp.[29] The full length protein contains only a small core region flanked by the typical, conserved terminal domains and is comprised of 439 amino acids in total. Strikingly, the core domain lacks the usual repetitive character and also the typical sequence motifs. Because of its low molecular weight, the newly identified protein has been called MaSp1s (MaSp1 short).[29]

In order to analyze the features of this novel type of major ampullate spidroins, MaSp1s was genetically engineered for recombinant production in *E. coli*. The gained eMaSp1s was

Received: January 19, 2017
Revised: February 20, 2017
Published: February 24, 2017

   DOI: 10.1021/acs.biomac.7b00090

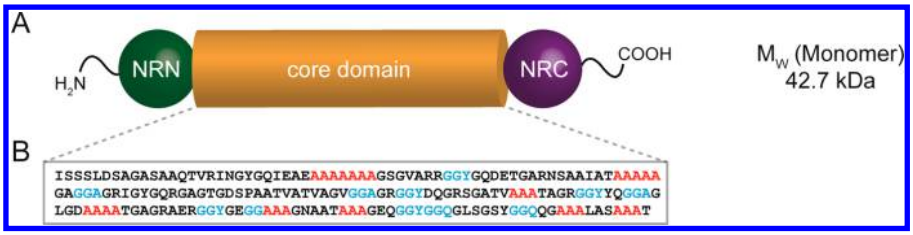

Figure 1. Schematic structure and core sequence of MaSp1s. (A) MaSp1s consists of a 191 aa long core domain flanked by a nonrepetitive amino- (NRN) and carboxy-terminal (NRC) domain. The theoretical molecular weight (MW, calculated using the ProtParam tool: http://web.expasy.org/protparam) is 42.7 kDa. (B) Sequence of the eMaSp1s core domain. MaSp1 specific sequence motifs are highlighted in red (poly-A) and blue (GGX). One unusual feature is the absence of the typically occurring repeats of sequence motifs. Another feature is the high content of charged amino acid residues (10.5%).

characterized concerning its secondary structure in solution as well as its thermal and chemical stability. Fibers were produced using wet-spinning, showing the versatility of this protein for the production of fibrous morphologies. Their mechanical data were compared to that of natural spider silk fibers and other wet-spun spider silk fibers, providing further insights into the basis of spider silk's mechanics.

MATERIALS AND METHODS

All chemicals used in this study had analytical grade purity and were acquired from Carl Roth GmbH & Co. KG (Karlsruhe, Germany). Double-distilled water was prepared using a Millipore system (Merck Millipore, Darmstadt, Germany).

Protein Production and Purification. Synthetic genes encoding the MaSp1s core domain and the terminal domains of *L. hesperus* NRN1 and NRC1 were obtained from Eurofins Genomics (Ebersberg, Germany). Cloning of the eMaSp1s (engineered MaSp1s) full length construct (NRN1, MaSp1s core domain, NRC1, 42.7 kDa) was performed using the pCS-system as previously described.[12] For gene expression, the construct was cloned into a pET-Vector containing a SUMO-TAG,[30,31] and the resulting vector was transformed into *E. coli* BL21(DE3)-gold (Novagen, Merck, Darmstadt, Germany). Gene expression was induced at OD_{600} = 50 using 0.1 mM IPTG followed by further 3 h of fermentation in a Minifors reactor (Infors HT, Bottmingen, Switzerland) at 30 °C in LB Medium containing 35 μg mL^{-1} kanamycin and 0.001% (v/v) Breox FMT 30 antifoam (Cognis, BASF, Ludwigshafen, Germany). Resulting cell pellets were disrupted using a high-pressure homogenizator (HDH Niro Soavi Panda 2K, Gea Niro Soavi, Parma, Italy) followed by centrifugation and addition of 10 mM imidazole to the supernatant. Protein purification was performed using an ÄKTA FPLC system (GE Healthcare, Germany). The supernatant was loaded onto an Ni-NTA sepharose column (120 mL, GE Healthcare, Germany) and washed with 50 mM Tris/HCl, 100 mM NaCl, 10 mM imidazole, pH 7.5 (buffer A) until the baseline was reached. A washing step with 30 mM imidazole (6% buffer B) before elution with 60% buffer B (50 mM Tris/HCl, 100 mM NaCl, 500 mM imidazole, pH 7.5) increased the purity of the protein. The eluate was mixed with 1:500 (v/v) SUMO-Protease (7 mg mL^{-1}) to cleave off the SUMO-TAG within 1 h at 20 °C and afterward eMaSp1s was precipitated using 20% ammonium sulfate at 4 °C for 1 h. After centrifugation, the resulting pellet was washed with water, dissolved in 6 M guanidinium thiocyanate, dialyzed against 25 mM NH_4HCO_3, and lyophilized.

$N1L(AQ)_{12}NR_3$ was used as a well-described spider silk protein control and produced using the SUMO-system[30,31] and purified using nickel affinity chromatography, followed by cleavage of the SUMO-TAG and ammonium sulfate precipitation as described previously.[12,27] $N1L(AQ)_{12}NR_3$ consists of 12 repetitive consensus modules, containing spider silk typical (MaSp2-type) polyalanine stretches (A) and glycine/proline-rich areas, flanked by N-and C-terminal domains (Figure S1).

Circular Dichroism (CD) and Fourier Transformed Infrared Spectroscopy (FTIR). CD measurements were performed using a Jasco J-715 spectropolarimeter (Jasco, Groß-Umstadt, Germany). For near-UV (70 μM protein concentration) and far-UV CD measurements (5 μM protein concentration), 10 mM sodium phosphate buffer, pH 7.5, and cuvettes with a path length of 0.5 cm (near-UV) and 0.1 cm (far-UV) were used, respectively. Thermal transitions (5 μM protein concentration) were measured at 222 nm and a heating rate of 1 °C min^{-1}. Chemical unfolding (5 μM protein concentration) was analyzed in the presence of increasing amounts of urea until a concentration of 7.5 M was reached. Samples were incubated for 5 h at 4 °C and analyzed at 222 nm.

FTIR measurements were recorded in absorbance mode using a Bruker Tensor 27 IR spectrometer (Bruker, Germany). Lyophilized samples were placed on an ATR-crystal and pressed with a stamp. Fibrous samples were measured with the attached hyperion 1000 microscope unit. Each measurement comprised a 60-scan interferogram with a 2 cm^{-1} resolution between 4000 and 800 cm^{-1}. The amide I region (1590−1720 cm^{-1}) was analyzed by Fourier self-deconvolution (FSD) using OPUS software (version 6.5). Signals were assigned to protein secondary structure elements according to Hu et al.[32]

Shear-Induced Fiber Assembly. The protein was directly solved in buffer containing 20 mM potassium phosphate, pH 7.5, and the final concentration was adjusted to 23.4 μM eMaSp1s. Samples were incubated for 16 h at 25 °C in 2 mL reaction tubes with overhead rotation at 21 rpm (Intellimixer RM-2, NeoLab, Germany). After rotation, clearly visible fibrous protein structures were analyzed on glass slides by optical microscopy using a Leica Microscope DMI 3000B.

Spinning Dope Preparation and Wet-Spinning. eMaSp1s and $N1L(AQ)_{12}NR3$ were wet-spun according to the protocol of Heidebrecht et al.[27] Blend fibers were spun using self-assembled, phase-separated (biomimetic) spinning dope. To generate a biomimetic spinning dope (BSD), both proteins were dissolved in 6 M GdmSCN and dialyzed separately against 50 mM Tris/HCl, pH 8.0, 100 mM NaCl buffer, which initiated refolding of the α-helical terminal domains, and mixed at a molar ratio of 1:1, followed by dialysis against 40 mM potassium phosphate buffer, pH 7.2.

MaSp1s fibers were spun using a classical spinning dope because it did not phase-separate in the absence of $N1L(AQ)_{12}NR3$. For preparation of a classical spinning dope (CSD), MaSp1s was dissolved in 6 M GdmSCN and dialyzed against 50 mM Tris/HCl, pH 8.0, 100 mM NaCl, followed by dialysis against 20% (w/v) PEG (35 kDa) solution up to a final spinning dope protein concentration of 10−12% (w/v).

The spinning dopes were extruded into an isopropanol/water coagulation bath at a speed of 5−7 μL min^{-1}. Poststretching was performed manually in isopropanol.

Fiber Analysis. Fiber morphology and fiber diameters were analyzed using an optical microscope (Leica DMI3000B) and the software Leica V4.3. SEM pictures of platinum sputtered samples (2 nm platinum coating) were taken using a Zeiss 1540 EsB CrossBeam (Carl Zeiss, Oberkochen, Germany).

Tensile Testing. For tensile testing, 1 cm long fibers were fixed on plastic sample holders with a 2 mm gap using superglue (UHU GmbH & Co. KG). Tensile testing was performed using a BOSE Electroforce 3220 with a 0.49 N load cell and a pulling rate of 0.04 mm s^{-1} at 20 °C

DOI: 10.1021/acs.biomac.7b00090

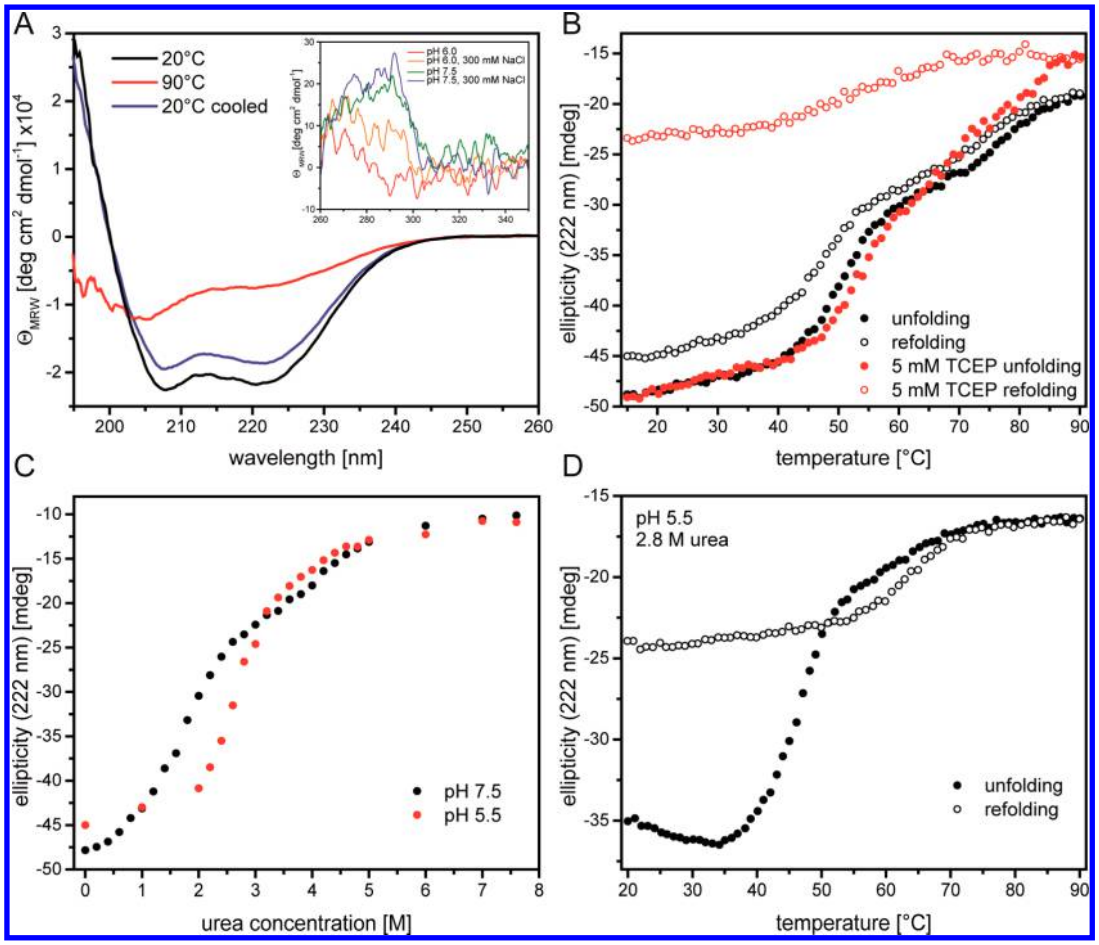

Figure 2. Structural characterization and thermal and chemical stability of eMaSp1s. (A) Far-UV spectra of eMaSp1s show mainly α-helical structure in solution. The inset shows the detected differences in near-UV spectra of eMaSp1s at pH 6.0 and pH 7.5 in the absence and presence of 300 mM NaCl. The far-UV spectra are indistinguishable at different pH values. (B) Thermal stability of eMaSp1s and influence of TCEP (tris(2-carboxyethyl)phosphine) as a reducing agent on thermal stability. (C) Urea-induced unfolding of eMaSp1s at pH 7.5 and pH 5.5. (D) Thermal stability of eMaSp1s at pH 5.5 in the presence of 2.8 M urea.

and 30% relative humidity (Bose Co., Framingham, MA). The cross-sectional area was calculated upon measuring the microfiber diameter at 5−10 different positions using optical microscopy. Mechanical data were calculated considering true stress and true strain using Microsoft Excel 2016 (Microsoft Corporation, Redmond, WA). Sample numbers were ≥15 except for unstretched eMaSp1s fibers spun from CSD (n = 6).

RESULTS AND DISCUSSION

Cloning, Production, and Purification of eMaSp1s. The sequence of a novel type of major ampullate spidroin, MaSp1s, comprises of 439 amino acids (aa) with a core domain (192 aa) flanked by spider silk-typical amino- (149 aa) and carboxy-terminal (98 aa) domains (Figure 1A).[29] The novel spidroin was attributed to the class of MaSp1 proteins, because MaSp1 characteristic motifs, such as GGX and polyalanine, and no proline residues were present (Figure 1B).[8] However, the identified sequence differed significantly from that of other major ampullate spidroins, because the detected polyalanine stretches were rather short and inhomogeneously distributed, and likewise GGX-motifs were sparsely found. The most striking difference to all preliminary known spidroins is its small, nonrepetitive core and the relatively large number of charged amino acid residues. In contrast, in comparison with terminal domains of various other spider silk proteins those of MaSp1s are highly conserved (Figure S2 in Supporting Information). To analyze the features of the MaSp1s core domain in comparison to those of "classical" ones, it was fused to the well-established and characterized terminal domains of *L. hesperus* MaSp1 (NRN1 and NRC1).[7,24,28]

After successful cloning, eMaSp1s was produced using the SUMO system, containing a polyhistidine affinity tag.[30] Highest yield and purity were achieved upon affinity chromatography, followed by SUMO-TAG cleavage, ammonium sulfate precipitation, and freeze drying. Final protein yield for MaSp1s after purification was in a range of 300−400 mg per liter of induced culture medium. For further experiments, the lyophilized protein was redissolved directly in aqueous buffers up to a concentration of 2% (w/v). The excellent solubility of the lyophilized protein in aqueous buffers was very likely due to its high amount of charged amino acid residues. Less charged MaSp derivatives often show lower yields in the range of 4−150 mg per liter[33] and have to be dissolved in strong denaturants (e.g., GdmSCN) after lyophilization and then dialyzed against aqueous buffers.[12,27]

Structural Characterization of eMaSp1s. eMaSp1s was structurally examined in solution using CD spectroscopy, and further its thermal and chemical stability was analyzed. Recent studies showed α-helical structure of terminal spider silk domains, whereas the core domains of spider silk proteins were

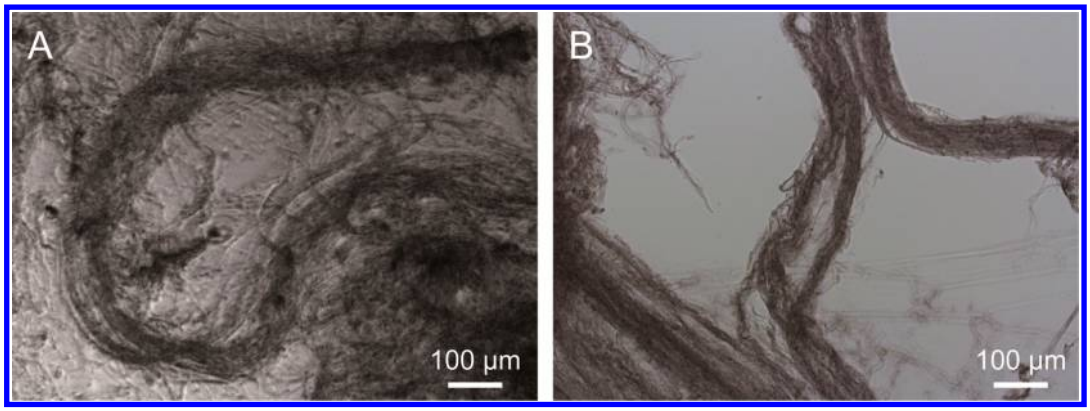

Figure 3. MaSp1s and N1L$(AQ)_{12}$NR3 fiber morphologies upon shear-induced assembly. Light microscopy of (A) eMaSp1s and (B) N1L$(AQ)_{12}$NR3 fibers assembled by rotation.

predicted to be mainly unfolded in solution.[34] In aqueous solution, eMaSp1s exists as a dimer, based on the fact that the C-terminal domain builds a permanent parallel-oriented dimer, covalently linked by a disulfide bond. eMaSp1s spectra showed local minima at 208 and 222 nm, indicative of mainly α-helical structures as expected for the terminal domains. At 90 °C, the protein was unfolded but it could refold almost completely upon cooling (Figure 2A).

Temperature-induced unfolding of eMaSp1s revealed a 2-step transition with melting temperatures (T_m) at 47 and 72 °C (Figure 2B), perfectly matching the melting points of the individual N- and C-terminal domains.[24,26] Refolding also occurred in a two-step process in the presence of reducing agents like TCEP during temperature-induced unfolding. A strong tendency of protein aggregation could be detected during refolding under reducing conditions due to destabilization of the C-terminal domain upon reducing its disulfide bond (Figure 2B).

Features of the near-UV CD spectra of eMaSp1s were similar to that of the isolated N-terminal domain (Figure 2A insert).[24] Significant differences could be observed for spectra at pH 7.5 (condition in the gland) and pH 6.0 (condition in the spinning duct) with a stronger influence of salt at pH 6.0 indicating a pH-dependent conformational switch as observed previously for the N-terminal domain. Taken together, the eMaSp1s solution structure is apparently dominated by the folded terminal domains with little structural impact of the core domain.

The chemical stability of eMaSp1s was tested in the presence of urea, revealing again a 2-step transition upon rising urea concentrations based on successive unfolding of both terminal domains (Figure 2C). In eMaSp1s, the N-terminal domain unfolds at urea concentrations of about 1.9 M, while the C-terminal domain unfolds at a concentration of about 3.6 M. Between these values at the transition point at 2.8 M urea, the N-terminal domain is unfolded but the C-terminal domain is still folded.

During natural fiber assembly, the pH value drops from pH 7.2 to pH 5.7,[35,36] however NRN is already a stable dimer at pH 6.0.[28,37] Chemical unfolding experiments of eMaSp1s at pH 5.5 clearly indicated a higher structural stability of NRN at lower pH values (Figure 2C). This is in accordance with previous results showing that the NRN domains form antiparallel homodimers at a slightly acidic pH value that stabilizes the structure.[24,38,39]

Temperature-induced unfolding of eMaSp1s at the chemical transition point of 2.8 M urea and at pH 5.5 showed a similar unfolding behavior as seen in the absence of urea but refolding led to aggregation of the protein due to destabilization of intermolecular salt bridges within the C-terminal domain at this pH (Figure 2D).[26]

Effect of Shear Forces on eMaSp1s Assembly. Shear stress is one of the main triggering factors of silk fiber assembly, which is accompanied by an increase in ß-sheet structure of the underlying proteins.[40−44]

Surprisingly, despite the high solubility of eMaSp1s in aqueous buffers at pH 7.5, which is negatively charged at these conditions, exposing a solution of recombinantly produced eMaSp1s to shear forces lead to clearly visible fibrils within the reaction tube after 16 h (Figure 3A). Such behavior was previously reported for other engineered spider silk proteins containing NRC domains (Figure 3B), while spidroins without NRC domains aggregated unspecifically.[40,45,46] Another previously described miniature spider silk protein derived from *Euprosthenops australis* (4RepCT) showed the same behavior.[25,46,47] In contrast to eMaSp1s with its novel nonrepetitive core domain, this 23.4 kDa protein consists of four repetitive modules containing polyalanine and glycine-rich stretches with two positive charges (Arg) and the conserved C-terminal domain of *Nephila clavipes*. The 4RepCT protein was merely spun into fibers by gently tilting a protein solution in glass tubes.[46]

Control fibers are shown exemplarily of the previously established N1L$(AQ)_{12}$NR3, a 76 kDa MaSp2 protein consisting of 12 repetitive consensus sequence modules of the core domain of *Araneus diadematus* fibroin 3 (ADF3), containing polyalanine stretches (A) and glycine/proline-rich areas (Q) but no charged amino acid residues and flanked by a respective N- and C-terminal domain (Figure 3B).[27] Rotation-induced self-assembled N1L$(AQ)_{12}$NR3 fibers had a diameter of 5−10 μm.

The diameter of individual rotation-induced self-assembled eMaSp1s fibers were slightly below 10 μm. It was not possible to determine their mechanical properties due to the instability of the fibers after the removal from the solution and the impossibility to isolate single fibers out of the resulting fiber bundles. Therefore, those fibers were not further investigated in this project, and another technique to produce fibers was evaluated.

Wet-Spinning. A large variety of artificial MaSp1 and MaSp2 proteins with differing molecular weight have been

DOI: 10.1021/acs.biomac.7b00090

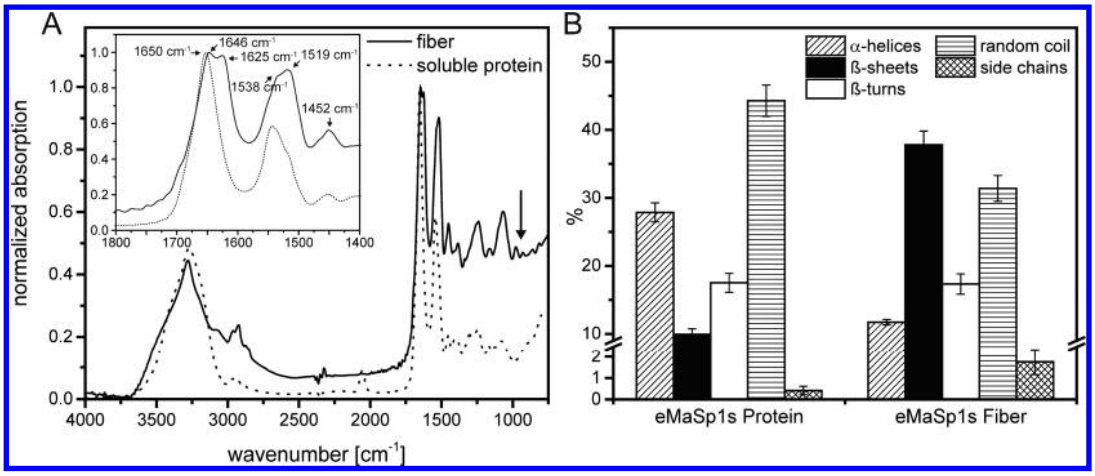

Figure 4. (A) Fourier-transformed infrared spectra of soluble eMaSp1s and eMaSp1s fibers. The inset shows the amide I and II regions between 1800 and 1400 cm^{-1} in more detail. (B) Secondary structure distribution of eMaSp1s in solution and eMaSp1s fibers. Spectra were deconvoluted using Fourier self-deconvolution (FSD) of the amide I band.[52]

produced using wet-spinning methods, and the challenge has been so far to obtain fibers with mechanical properties comparable to that of natural spider silk fibers.[27,33]

All proteins in this study contained the folded amino- and carboxy-terminal domains, shown to be important for spider silk assembly properties.[27] The N-terminal domain is monomeric under neutral pH conditions, likely inhibiting protein aggregation within the spinning dope. The C-terminal domain is a stable disulfide-bridged dimer, crucial for protein assembly into micellar structures within the spinning dope. Furthermore, both domains seem to be important for initiating fiber assembly upon external stimuli such as pH-drop and shear-forces.

The preparation of spinning dopes followed two routes: a classical one by simply concentrating spidroin solutions and a more recent one depending on self-assembly of the spidroins prior to spinning (yielding a so-called biomimetic spinning dope). In the biomimetic spinning dope, a phase separation is caused by a conformational change of the NRC-domain, effecting the spidroins to assemble into micelle-like structures.[48]

Interestingly, eMaSp1s showed no phase separation probably due to the sequence (short length, changed amino acids) of the core domain. According to the current model, the core domain is packed inside the spidrion micelles (existing in the spinning dope), while the terminal domains reside on their surface. The underlying driving force is based on the more hydrophobic character of the core domain in combination with its larger proportion in comparison to the terminal domains. The short length in combination with the solubility (hydrophobicity index: −0.1) of the eMaSp1s core domain probably does not support this molecular feature.

Therefore, eMaSp1s was spun from classical spinning dope. Wet-spinning of soluble eMaSp1s (15% (w/v)) out of an aqueous buffer solution into isopropanol/water mixture was successful, and fibers could be poststretched in isopropanol up to 400% (Figure 5A insert).

In addition, eMaSp1s could be blended with N1L-$(AQ)_{12}$NR3, which can phase separate,[27] at a molar ratio of 1:1. Phase separation of this blend was possible and yielded the above-mentioned biomimetic spinning dope. Interestingly, under these conditions eMaSp1s could be implemented into the micelles (Figure 6) and in the fibers spun thereof, as seen by gel electrophoresis (Figure S3). As-spun blend fibers could be poststretched up to at least 600% (Figure 5B insert) similar to fibers made solely of N1L$(AQ)_{12}$NR3.

Structural Properties of eMaSp1s Fibers. Upon spidroin assembly, a conformational transition of the core domain of the underlying proteins occurs: intrinsically unstructured regions fold into ß-sheets, which are responsible for the strength of the fibers.[17,49] In case of eMaSp1s, the FTIR-absorbance maximum of soluble protein at 1650 cm^{-1} (α-helical structure) shifted to an IR-absorbance maximum at 1625 cm^{-1} in eMaSp1s fibers, characteristic for ß-sheet structures (Figure 4A). Accordingly, the signal at 1519 cm^{-1} was significantly enhanced, reflecting a further indication for the formation of ß-sheets. However, because eMaSp1s does not contain the typical polyalanine stretches of MaSp, which are normally responsible for ß-sheet formation, the ß-sheets were likely based on the less "perfect" alanine-rich sequences, as identified in a secondary structure prediction analysis of the eMaSp1s core domain, based on the method of Chou and Fasman (Figure S4).[50] Structure prediction models are based on soluble proteins in which alanine-rich sequences predominantly form α-helices, while they convert into ß-sheet structures in silk proteins upon assembly.

Because the polyalanine stretches of eMaSp1s are, unlike in other spidroins, imperfect, no specific polyalanine stacking and related IR-peak for ß-ala at 963 cm^{-1} could be detected (arrow in Figure 4A).[51]

The overall secondary structure content was calculated using FSD analysis (Figure 4B), confirming an increase of the ß-sheet content from 10% in solution to 38% in fibers. The α-helical content decreased from 28% to 12%, and the random coil content from 44% to 31%.

Mechanical Properties of eMaSp1s and eMaSp1s/N1L$(AQ)_{12}$NR3 Blend Fibers. Stress−strain curves were analyzed of eMaSp1s and N1L$(AQ)_{12}$NR3 fibers spun from classical spinning dopes (CSD) and eMaSp1s/N1L$(AQ)_{12}$NR3 blend fibers (ratio 1:1) spun from prestructured biomimetic dopes (BSD) and compared to that of natural spider silk fibers.

eMaSp1s fibers (CSD) could be poststretched up to 400% (average diameter after poststretching: 49 ± 7 μm), whereas N1L$(AQ)_{12}$NR3 fibers (CSD) could be stretched up to at least 600% (average diameter after poststretching: 39 ± 9 μm). Surprisingly, mechanical properties of as-spun and post-stretched eMaSp1s fibers were slightly better than that of

DOI: 10.1021/acs.biomac.7b00090

Table 1. Mechanical Properties of Natural and Different As-Spun and Post-Stretched Recombinant Spider Silk Fibers Spun from Classical Spinning Dopes and Biomimetic Spinning Dopes[a]

	classical spinning dope			
	N1L(AQ)$_{12}$NR3		eMaSp1s	
poststretching [%]	0	600	0	400
diameter [μm]	75 ± 12	39 ± 9	77 ± 7	49 ± 7
extensibility [%]	4 ± 2	109 ± 23	4 ± 1	102 ± 24
strength [MPa]	25 ± 14	206 ± 68	31 ± 7	282 ± 66
toughness [MJm^{-3}]	0.8 ± 0.4	116 ± 46	0.9 ± 0.2	144 ± 44
Young's modulus [GPa]	0.3 ± 0.2	1.3 ± 0.7	0.9 ± 0.1	1.5 ± 0.3

	biomimetic spinning dope				
	N1L(AQ)$_{12}$NR3		MaSp1s/N1L(AQ)$_{12}$NR3 blend		natural dragline silk[27]
poststretching [%]	0	600	0	600	
diameter [μm]	155 ± 8	27 ± 10	66 ± 17	36 ± 9	4 ± 0.4
extensibility [%]	6 ± 1	110 ± 25	8 ± 2	93 ± 18	24 ± 8
strength [MPa]	13 ± 2	370 ± 59	23 ± 9	316 ± 103	1183 ± 334
toughness [MJm^{-3}]	0.3 ± 0.1	189 ± 33	0.8 ± 0.1	142 ± 50	167 ± 65
young's modulus [GPa]	0.5 ± 0.1	4 ± 1	0.8 ± 0.2	1 ± 0.4	8 ± 2

[a]Tensile testing was performed at 20°C and 30% RH. Sample numbers were ≥15 except for unstretched eMaSp1s fibers spun from CSD (n = 6).

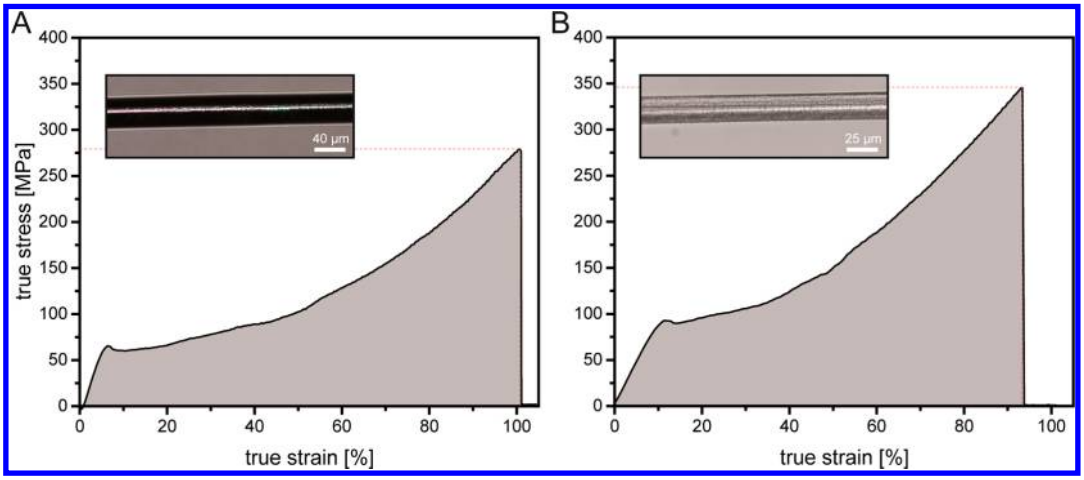

Figure 5. (A) True stress−strain curve of a 400% poststretched eMaSp1s fiber (CSD) (inset: light microscopy image). (B) True stress strain curve of a 600% post stretched wet-spun fiber (inset: light microscopy image) composed of a blend of eMaSp1s and N1L(AQ)$_{12}$NR3 at a 1:1 ratio (BSD).

N1L(AQ)$_{12}$NR3 fibers spun from classical spinning dopes. While showing the same extensibility (102 ± 24%), eMaSp1s fibers showed a slightly higher stiffness and higher strength (282 ± 66 MPa), resulting in a slightly but significantly higher overall toughness (144 ± 44 MJm^{-3}) (Table 1A, Figure 5A). The slightly better mechanics of eMaSp1s fibers in comparison to that of N1L(AQ)$_{12}$NR3 fibers are most likely based on a higher overall alanine content (29% vs 16%) and the presence of 22 (11.5%) charged amino acids (resulting in ionic interactions, generally exceeding the strength of covalent ones)[53,54] in its core domain, while N1L(AQ)$_{12}$NR3 lacks charges.

Taken together, mechanical properties of fibers were high, regardless of which core was used. Former studies revealed mechanical properties of spider silk fibers to be dependent on the molecular weight and amino acid sequence composition of the underlying protein core domain.[6,8,55,56]

Despite the different molecular setup of the core domains of eMaSp1s and N1L(AQ)$_{12}$NR3 (in terms of molecular weight, charges, and amino acid composition), our results show that the influence of the controlling terminal domains is of particular importance for fiber assembly at aqueous conditions.

In terms of extensibility, strength, and toughness, blend fibers were slightly inferior to those made of plain N1L(AQ)$_{12}$NR3 (Table 1B, Figure 5B), being in line with former results of MaSp1/MaSp2 blend fibers.[56] Integration of eMaSp1s seems to interfere with N1L(AQ)$_{12}$NR3 assembly, intercalating in its structure and thereby preventing a perfect intramolecular alignment of the (AQ)$_{12}$ core domain during fiber assembly.

CONCLUSION

eMaSp1s has been successfully engineered and recombinantly produced in *E. coli*. Circular dichroism analysis of the protein revealed the dominance of its helically folded terminal domains in solution, whereas eMaSp1s fibers showed an increased ß-sheet content as shown by FTIR spectroscopy.

Previous studies investigating the mechanical properties of wet-spun fibers made from different recombinantly produced spider silk proteins containing none, only one, or both terminal domains based on sequences of *Araneus diadematus* fibroin 3 (ADF3), named eADF3 (AQ)$_n$ underline the significant effect of both terminal domains on fiber assembly and resulting mechanical properties.

DOI: 10.1021/acs.biomac.7b00090

Here, we varied the protein core domain, replacing the eADF3 $(AQ)_n$ core domain by the novel 17 kDa MaSp1s core domain. Figure 6 outlines the most probable morphological differences in spinning dope conformation, phase separation properties and resulting putative fiber structures. Our data support the conclusion that the controlling function of the terminal domains during spinning dope preparation and spidroin assembly is as important as the sequence or the molecular weight of the core domain.

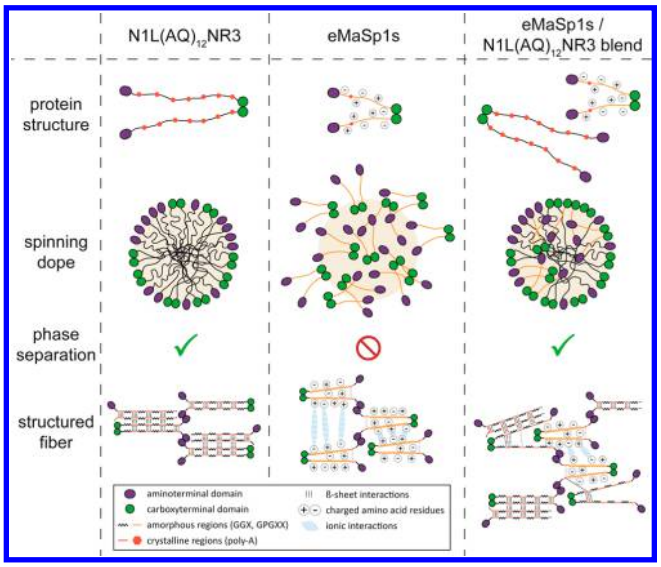

Figure 6. Schematic overview of structure and assumed morphologies of spidroins differing in molecular weight and sequence of their core domain and blends made thereof. N1L$(AQ)_{12}$NR3 consists of a highly repetitive hydrophobic core with 47 kDa, and eMaSp1s of a small nonrepetitive core (17 kDa) with 22 charged amino acids, inhibiting the prearrangement into micelles (no phase separation). Mechanical properties of resulting fibers are mainly based on ß-sheet packing and terminal domain interactions. In a 1:1 blend, eMaSp1s is able to incorporate into N1L$(AQ)_{12}$NR3 micelles but interferes with a precise alignment of the $(AQ)_{12}$ core domain, yielding slightly decreased mechanical properties.

The found features open the road for further studies, replacing the protein core domain with other spider silk core motifs with different length, charge, and molecular setup or even completely artificial ones, possibly yielding fibers with new properties depending on the respective core domain.

■ ASSOCIATED CONTENT

Supporting Information

The Supporting Information is available free of charge on the ACS Publications website at DOI: 10.1021/acs.biomac.7b00090.

Amino acid sequences of N1L$(AQ)_{12}NR_3$ molecules (Figure S1). Sequence comparison of NRN and NRC domains of MaSp of different spider species (Figure S2). Coomassie-stained SDS-gel analysis of eMaSp1s, N1L-$(AQ)_{12}$NR3, and a resolved wet-spun blend fiber made of both proteins (Figure S3). Sequence and secondary structure prediction of the eMaSp1s core domain (Figure S4) (PDF)

■ AUTHOR INFORMATION

Corresponding Author

*E-mail: thomas.scheibel@bm.uni-bayreuth.de.

ORCID

Thomas Scheibel: 0000-0002-0457-2423

Author Contributions

Conceptualization, C.T. and T.S.; investigation, C.T.; writing (original draft), C.T.; writing (review and editing), T.S.; visualization, C.T.; supervision, T.S..

Notes

The authors declare no competing financial interest.

■ ACKNOWLEDGMENTS

Funding was provided by EFRE Ziel ETZ Freistaat Bayern – Tschechien Projekt Nr. 123.

■ REFERENCES

(1) Rising, A.; Nimmervoll, H.; Grip, S.; Fernandez-Arias, A.; Storckenfeldt, E.; Knight, D. P.; Vollrath, F.; Engstrom, W. Spider silk proteins–mechanical property and gene sequence. *Zool. Sci.* **2005**, *22* (3), 273–81.

(2) Gosline, J. M.; Guerette, P. A.; Ortlepp, C. S.; Savage, K. N. The mechanical design of spider silks: from fibroin sequence to mechanical function. *J. Exp Biol.* **1999**, *202* (Pt 23), 3295–303.

(3) Hu, X.; Vasanthavada, K.; Kohler, K.; McNary, S.; Moore, A. M.; Vierra, C. A. Molecular mechanisms of spider silk. *Cell. Mol. Life Sci.* **2006**, *63* (17), 1986–99.

(4) Blackledge, T. A.; Summers, A. P.; Hayashi, C. Y. Gumfooted lines in black widow cobwebs and the mechanical properties of spider capture silk. *Zoology (Munich, Ger.)* **2005**, *108* (1), 41–6.

(5) Blackledge, T. A.; Perez-Rigueiro, J.; Plaza, G. R.; Perea, B.; Navarro, A.; Guinea, G. V.; Elices, M. Sequential origin in the high performance properties of orb spider dragline silk. *Sci. Rep.* **2012**, *2*, 782.

(6) Madurga, R.; Blackledge, T. A.; Perea, B.; Plaza, G. R.; Riekel, C.; Burghammer, M.; Elices, M.; Guinea, G.; Perez-Rigueiro, J. Persistence and variation in microstructural design during the evolution of spider silk. *Sci. Rep.* **2015**, *5*, 14820.

(7) Ayoub, N. A.; Garb, J. E.; Tinghitella, R. M.; Collin, M. A.; Hayashi, C. Y. Blueprint for a high-performance biomaterial: full-length spider dragline silk genes. *PLoS One* **2007**, *2* (6), e514.

(8) Hayashi, C. Y.; Shipley, N. H.; Lewis, R. V. Hypotheses that correlate the sequence, structure, and mechanical properties of spider silk proteins. *Int. J. Biol. Macromol.* **1999**, *24* (2–3), 271–5.

(9) Sponner, A.; Schlott, B.; Vollrath, F.; Unger, E.; Grosse, F.; Weisshart, K. Characterization of the protein components of Nephila clavipes dragline silk. *Biochemistry* **2005**, *44* (12), 4727–36.

(10) Andersen, S. O. Amino acid composition of spider silks. *Comp. Biochem. Physiol.* **1970**, *35* (3), 705–711.

(11) Xu, M.; Lewis, R. V. Structure of a protein superfiber: spider dragline silk. *Proc. Natl. Acad. Sci. U. S. A.* **1990**, *87* (18), 7120–4.

(12) Huemmerich, D.; Helsen, C. W.; Quedzuweit, S.; Oschmann, J.; Rudolph, R.; Scheibel, T. Primary structure elements of spider dragline silks and their contribution to protein solubility. *Biochemistry* **2004**, *43* (42), 13604–12.

(13) Hinman, M. B.; Lewis, R. V. Isolation of a clone encoding a second dragline silk fibroin. Nephila clavipes dragline silk is a two-protein fiber. *J. Biol. Chem.* **1992**, *267* (27), 19320–4.

(14) Brooks, A. E.; Steinkraus, H. B.; Nelson, S. R.; Lewis, R. V. An investigation of the divergence of major ampullate silk fibers from Nephila clavipes and Argiope aurantia. *Biomacromolecules* **2005**, *6* (6), 3095–9.

(15) Hayashi, C. Y.; Blackledge, T. A.; Lewis, R. V. Molecular and mechanical characterization of aciniform silk: uniformity of iterated sequence modules in a novel member of the spider silk fibroin gene family. *Mol. Biol. Evol.* **2004**, *21* (10), 1950–1959.

(16) Guerette, P. A.; Ginzinger, D. G.; Weber, B. H.; Gosline, J. M. Silk properties determined by gland-specific expression of a spider fibroin gene family. *Science* **1996**, *272* (5258), 112−5.
(17) Simmons, A. H.; Michal, C. A.; Jelinski, L. W. Molecular orientation and two-component nature of the crystalline fraction of spider dragline silk. *Science* **1996**, *271* (5245), 84−87.
(18) Perez-Rigueiro, J.; Elices, M.; Plaza, G. R.; Guinea, G. V. Similarities and differences in the supramolecular organization of silkworm and spider silk. *Macromolecules* **2007**, *40* (15), 5360−5365.
(19) Liu, Y.; Shao, Z.; Vollrath, F. Elasticity of spider silks. *Biomacromolecules* **2008**, *9* (7), 1782−6.
(20) Fahnestock, S. R.; Irwin, S. L. Synthetic spider dragline silk proteins and their production in Escherichia coli. *Appl. Microbiol. Biotechnol.* **1997**, *47* (1), 23−32.
(21) Hinman, M. B.; Jones, J. A.; Lewis, R. V. Synthetic spider silk: a modular fiber. *Trends Biotechnol.* **2000**, *18* (9), 374−9.
(22) Candelas, G. C.; Cintron, J. A Spider Fibroin and Its Synthesis. *J. Exp. Zool.* **1981**, *216* (1), 1−6.
(23) Motriuk-Smith, D.; Smith, A.; Hayashi, C. Y.; Lewis, R. V. Analysis of the conserved N-terminal domains in major ampullate spider silk proteins. *Biomacromolecules* **2005**, *6* (6), 3152−9.
(24) Hagn, F.; Thamm, C.; Scheibel, T.; Kessler, H. pH-dependent dimerization and salt-dependent stabilization of the N-terminal domain of spider dragline silk–implications for fiber formation. *Angew. Chem., Int. Ed.* **2011**, *50* (1), 310−3.
(25) Askarieh, G.; Hedhammar, M.; Nordling, K.; Saenz, A.; Casals, C.; Rising, A.; Johansson, J.; Knight, S. D. Self-assembly of spider silk proteins is controlled by a pH-sensitive relay. *Nature* **2010**, *465* (7295), 236−8.
(26) Hagn, F.; Eisoldt, L.; Hardy, J. G.; Vendrely, C.; Coles, M.; Scheibel, T.; Kessler, H. A conserved spider silk domain acts as a molecular switch that controls fibre assembly. *Nature* **2010**, *465* (7295), 239−42.
(27) Heidebrecht, A.; Eisoldt, L.; Diehl, J.; Schmidt, A.; Geffers, M.; Lang, G.; Scheibel, T. Biomimetic fibers made of recombinant spidroins with the same toughness as natural spider silk. *Adv. Mater.* **2015**, *27* (13), 2189−94.
(28) Bauer, J.; Schaal, D.; Eisoldt, L.; Schweimer, K.; Schwarzinger, S.; Scheibel, T. Acidic Residues Control the Dimerization of the N-terminal Domain of Black Widow Spiders' Major Ampullate Spidroin 1. *Sci. Rep.* **2016**, *6*, 34442.
(29) Han, L.; Zhang, L.; Zhao, T.; Wang, Y.; Nakagaki, M. Analysis of a new type of major ampullate spider silk gene, MaSp1s. *Int. J. Biol. Macromol.* **2013**, *56*, 156−61.
(30) Butt, T. R.; Edavettal, S. C.; Hall, J. P.; Mattern, M. R. SUMO fusion technology for difficult-to-express proteins. *Protein Expression Purif.* **2005**, *43* (1), 1−9.
(31) Marblestone, J. G.; Edavettal, S. C.; Lim, Y.; Lim, P.; Zuo, X.; Butt, T. R. Comparison of SUMO fusion technology with traditional gene fusion systems: enhanced expression and solubility with SUMO. *Protein Sci.* **2006**, *15* (1), 182−189.
(32) Hu, X.; Kaplan, D.; Cebe, P. Determining beta-sheet crystallinity in fibrous proteins by thermal analysis and infrared spectroscopy. *Macromolecules* **2006**, *39* (18), 6161−6170.
(33) Heidebrecht, A.; Scheibel, T. Recombinant production of spider silk proteins. *Adv. Appl. Microbiol.* **2013**, *82*, 115−53.
(34) Lefevre, T.; Boudreault, S.; Cloutier, C.; Pezolet, M. Diversity of molecular transformations involved in the formation of spider silks. *J. Mol. Biol.* **2011**, *405* (1), 238−53.
(35) Kronqvist, N.; Otikovs, M.; Chmyrov, V.; Chen, G.; Andersson, M.; Nordling, K.; Landreh, M.; Sarr, M.; Jornvall, H.; Wennmalm, S.; Widengren, J.; Meng, Q.; Rising, A.; Otzen, D.; Knight, S. D.; Jaudzems, K.; Johansson, J. Sequential pH-driven dimerization and stabilization of the N-terminal domain enables rapid spider silk formation. *Nat. Commun.* **2014**, *5*, 3254.
(36) Andersson, M.; Chen, G.; Otikovs, M.; Landreh, M.; Nordling, K.; Kronqvist, N.; Westermark, P.; Jornvall, H.; Knight, S.; Ridderstrale, Y.; Holm, L.; Meng, Q.; Jaudzems, K.; Chesler, M.; Johansson, J.; Rising, A. Carbonic anhydrase generates CO2 and H+ that drive spider silk formation via opposite effects on the terminal domains. *PLoS Biol.* **2014**, *12* (8), e1001921.
(37) Bauer, J.; Scheibel, T. Conformational Stability and Interplay of Helical N- and C-Terminal Domains with Implications on Major Ampullate Spidroin Assembly. *Biomacromolecules* **2017**, DOI: 10.1021/acs.biomac.6b01713.
(38) Landreh, M.; Askarieh, G.; Nordling, K.; Hedhammar, M.; Rising, A.; Casals, C.; Astorga-Wells, J.; Alvelius, G.; Knight, S. D.; Johansson, J.; Jornvall, H.; Bergman, T. A pH-dependent dimer lock in spider silk protein. *J. Mol. Biol.* **2010**, *404* (2), 328−36.
(39) Gaines, W. A.; Sehorn, M. G.; Marcotte, W. R., Jr. Spidroin N-terminal domain promotes a pH-dependent association of silk proteins during self-assembly. *J. Biol. Chem.* **2010**, *285* (52), 40745−53.
(40) Rammensee, S.; Slotta, U.; Scheibel, T.; Bausch, A. R. Assembly mechanism of recombinant spider silk proteins. *Proc. Natl. Acad. Sci. U. S. A.* **2008**, *105* (18), 6590−5.
(41) Cromwell, M. E.; Hilario, E.; Jacobson, F. Protein aggregation and bioprocessing. *AAPS J.* **2006**, *8* (3), E572−9.
(42) Vezy, C.; Hermanson, K. D.; Scheibel, T.; Bausch, A. R. Interfacial rheological properties of recombinant spider-silk proteins. *Biointerphases* **2009**, *4* (3), 43−6.
(43) Heim, M.; Keerl, D.; Scheibel, T. Spider silk: from soluble protein to extraordinary fiber. *Angew. Chem., Int. Ed.* **2009**, *48* (20), 3584−96.
(44) Dicko, C.; Kenney, J. M.; Vollrath, F. Beta-silks: enhancing and controlling aggregation. *Adv. Protein Chem.* **2006**, *73*, 17−53.
(45) Eisoldt, L.; Hardy, J. G.; Heim, M.; Scheibel, T. R. The role of salt and shear on the storage and assembly of spider silk proteins. *J. Struct. Biol.* **2010**, *170* (2), 413−9.
(46) Stark, M.; Grip, S.; Rising, A.; Hedhammar, M.; Engstrom, W.; Hjalm, G.; Johansson, J. Macroscopic fibers self-assembled from recombinant miniature spider silk proteins. *Biomacromolecules* **2007**, *8* (5), 1695−701.
(47) Hedhammar, M.; Rising, A.; Grip, S.; Martinez, A. S.; Nordling, K.; Casals, C.; Stark, M.; Johansson, J. Structural properties of recombinant nonrepetitive and repetitive parts of major ampullate spidroin 1 from Euprosthenops australis: implications for fiber formation. *Biochemistry* **2008**, *47* (11), 3407−17.
(48) Exler, J. H.; Hummerich, D.; Scheibel, T. The amphiphilic properties of spider silks are important for spinning. *Angew. Chem., Int. Ed.* **2007**, *46* (19), 3559−62.
(49) Lewis, R. V. Spider Silk - the Unraveling of a Mystery. *Acc. Chem. Res.* **1992**, *25* (9), 392−398.
(50) Chou, P. Y.; Fasman, G. D. Prediction of protein conformation. *Biochemistry* **1974**, *13* (2), 222−45.
(51) Papadopoulos, P.; Solter, J.; Kremer, F. Structure-property relationships in major ampullate spider silk as deduced from polarized FTIR spectroscopy. *Eur. Phys. J. E: Soft Matter Biol. Phys.* **2007**, *24* (2), 193−9.
(52) Kauppinen, J. K.; Moffatt, D. J.; Mantsch, H. H.; Cameron, D. G. Fourier Self-Deconvolution - a Method for Resolving Intrinsically Overlapped Bands. *Appl. Spectrosc.* **1981**, *35* (3), 271−276.
(53) Pauling, L. *The nature of the chemical bond and the structure of molecules and crystals; an introduction to modern structural chemistry*, 3d ed.; Cornell University Press: Ithaca, NY, 1960.
(54) Kumar, S.; Nussinov, R. Close-range electrostatic interactions in proteins. *ChemBioChem* **2002**, *3* (7), 604−17.
(55) Xia, X. X.; Qian, Z. G.; Ki, C. S.; Park, Y. H.; Kaplan, D. L.; Lee, S. Y. Native-sized recombinant spider silk protein produced in metabolically engineered Escherichia coli results in a strong fiber. *Proc. Natl. Acad. Sci. U. S. A.* **2010**, *107* (32), 14059−63.
(56) Brooks, A. E.; Nelson, S. R.; Jones, J. A.; Koenig, C.; Hinman, M.; Stricker, S.; Lewis, R. V. Distinct contributions of model MaSp1 and MaSp2 like peptides to the mechanical properties of synthetic major ampullate silk fibers as revealed in silico. *Nanotechnol., Sci. Appl.* **2008**, *1*, 9−16.